4.2 V Wearable Asymmetric Supercapacitor Devices Based on VO_x//MnO_x Electrode and Eco-friendly Deep Eutectic Solvent-Based Gel Electrolyte

Ming-Jay Deng,[1,2,]* Tzung-Han Chou,[2] Li-Hsien Yeh,[2,3,]* Jin-Ming Chen,[4,]* Kueih-Tzu Lu[4]

[1] *Bachelor Program in Interdisciplinary Studies, National Yunlin University of Science and Technology, Yunlin 64002, Taiwan*

[2] *Department of Chemical and Materials Engineering, National Yunlin University of Science and Technology, Yunlin 4002, Taiwan*

[3] *Department of Chemical Engineering, National Taiwan University of Science and Technology, Taipei 10607, Taiwan*

[4] *National Synchrotron Radiation Research Center, Hsinchu, Taiwan*

* Corresponding authors:

E-mail: martinez730523@yahoo.com.tw and dengmj@yuntech.edu.tw (Ming-Jay Deng); lhyeh@mail.ntust.edu.tw (Li-Hsien Yeh); jmchen@nsrrc.org.tw (Jin-Ming Chen)

Fabrication of nanoporous VO_x/PGP and MnO_x/PGP electrodes

The PGP electrode as a cleaned film (area ~6 cm^2) was pretreated by cleaning in ethanol (2 min), soaking in 0.3M HCl (10 min), rinsing with deionized water, and then drying in a fume cupboard at 27 °C. Metal-nucleation layers were produced on PGP substrates by a Pt sputtered coating of thickness ~100 nm. The Pt/PGP substrates were highly conducting (>1000 S/cm). A nanoporous VO_x layer was loaded onto the Pt/PGP substrate by electrochemical anodic deposition at 1.2 V in a mixture (volume ratio 1:1) of deionized water and ethanol containing 0.2 M $VOSO_4$ and 0.1 M $Na(CH_3COO)$ to assemble the nanoporous VO_x/PGP electrodes with a saturated calomel electrode (SCE) and a Pt counter electrode. The Ni-nanotube layer was prepared on a PGP substrate with electrodeposition at 27°C with a SCE and a Pt counter electrode. Firstly, Cu-Ni layers were electrodeposited from a plating solution (0.5 M $NiSO_4$, 0.5 M $NiCl_2$, 0.01 M $CuSO_4$, and1 M H_3BO_3). The deposition process was performed at 27°C in a three-electrode cell with a Pt counter electrode and a SCE. PGP electrode with area of ~6 cm^2 was assembled as the working electrode. Through the potential scan from the open circuit potential (~0 V) in a negative direction, the onset of the Cu reduction current at approximately –0.1 V was followed by a reduction peak associated with the nucleation and growth of Cu metal film. As Cu^{2+} has a limited mass transfer because of its small concentration, the deposition current varied tiny with potential until –0.75 V, at which point Ni^{2+} began reduction. At more negative potential, Cu and Ni were co-deposited. The anodic peak about 0.5 V is attributed to a selective dissolution of Cu from the Cu-Ni layers in the deposit. The co-deposition of Cu-Ni layers and then the selective etching of Cu from the deposit were completed in the same plating solution on exchanging the applied potential at –0.85 V and +0.55 V, respectively. The Cu-Ni layers were first coated on PGP electrode at –0.85 V; total deposited charge was 20 Coulomb. Electrochemical etching of Cu from the Cu-Ni layer was executed on exchanging the potential to +0.55 V until a current density 20 $\mu A/cm^2$ to develop the Ni-nanotube layer. Chemical segregation within deposited

Cu-Ni grains was observed by previous authors.[1,2] As a result, we have developed an efficient electrochemical technique to construct Ni-nanotube/PGP electrodes. The Ni-nanotube layer (excluding graphite or paper) loaded was on average 0.5 mg/cm^2 (XP105DR Mettler Toledo). MnO_x nanofiber layers were loaded onto the Ni-nanotube/PGP substrate by electrodeposition at 0.45 V in a solution containing 0.3 M $Mn(CH_3COO)_2$ (Sigma-Aldrich) and 0.1 M NH_4CH_3COO (Acros) at 27°C to assemble the nanoporous MO_x/PGP electrodes with a Pt counter electrode and a SCE. The typical mass of the deposited oxide, measured with a microbalance (XP105DR Mettler Toledo, accuracy 0.1 mg), was ~12 mg. The mass of dead components (electrolyte, conductive paper, separator) was not considered to active materials (MnO_x 2.0 mg/cm^2 and VO_x 2.0 mg/cm^2).

Electrochemical measurements

Electrochemical performances of VO_x/PGP and MnO_x/PGP electrodes were measured in KCl solution (1 M, 27 °C) using cyclic voltammetry (CV) with a Pt counter electrode and a SCE. A Pt wire immersed in PAL solution contained in a glass tube with porous Vycor tip (Bioanalytical Systems, MF-2042) was used as a quasi-reference electrode in $LiClO_4$−acetamide or PAL electrolyte systems. And the performances of VO_x/PGP and MnO_x/PGP electrodes in PAL electrolyte were measured with a Pt counter electrode and a quasi-reference electrode. An electrochemical impedance spectroscopy (EIS) experiment was studied using the frequency range from 0.1 Hz to 100 kHz with an amplitude of 5 mV. All electrochemical measurements were made with a potentiostat (AUTOLAB).

Calculation method

C_{sp} of cyclic voltammetry (CV) and galvanostatic charge-discharge (GCD) cycles in a three electrode system are calculated as follows,

$$C_{sp} = Q_{\mathrm{m}} / \Delta V \qquad (1)$$

$$C_{sp} = I \Delta \mathrm{t} / \Delta V w \qquad (2)$$

in which Q_m denotes the specific voltammetric charge ((based on mass of VO_x or MnO_x) integrated from CV, ΔV denotes the scanning range, I is applied current density (1–50 A/g), w is VO_x or MnO_x mass and Δt is duration of discharge cycling. With charge-discharge curves based on two electrode systems, C_{asy} is specific capacitance of an asymmetric supercapacitor, derived from GCD acquired by the equation $C_{asy} = I \Delta t / \Delta V W$, in which W ($W = w^+ + w^-$) means the total active material masses on both positive and negative electrodes. The energy density (E) and power density (P) are calculated from the GCD curves according to eqs 3 and 4,[3-5]

$$E = 1/2\ C_{asy} \Delta V^2 \qquad (3)$$

$$P = E / \Delta t \qquad (4)$$

in which ΔV is cell voltage (*i.e.* 4.2 V) and Δt is discharge time.

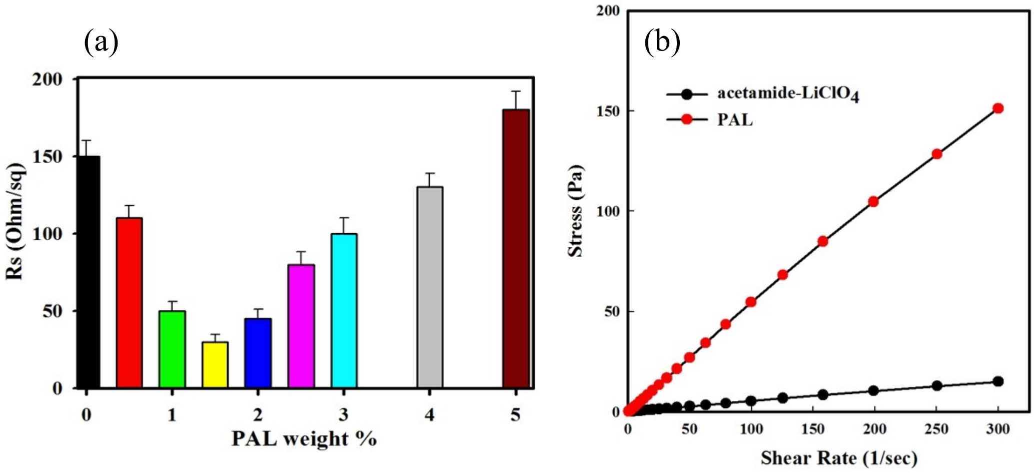

Figure S1. (a) Effect of addition of PAL gel to ink on the local sheet resistivity. The error ranges of all bars presented here are ±10%. (b) Shear rheometry data for the acetamide-$LiClO_4$ and PAL electrolyte.

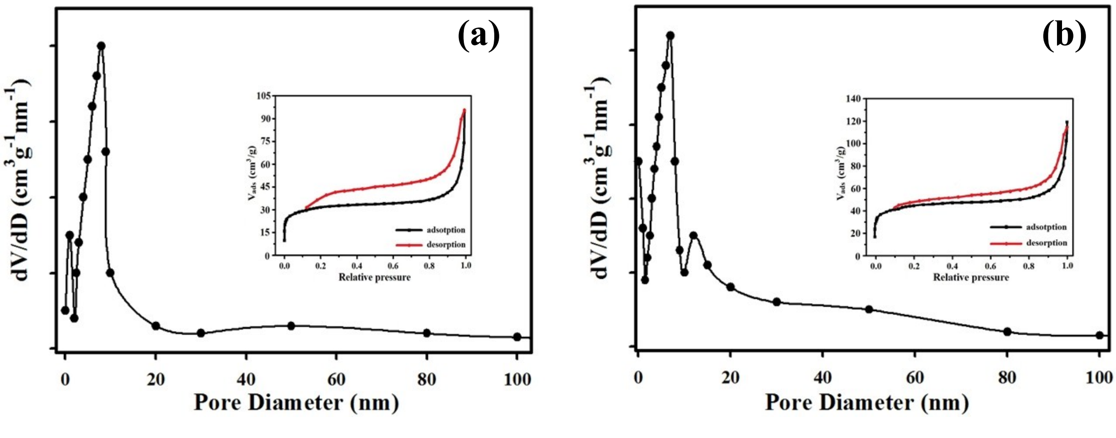

Figure S2. BJH pore size distributions of (a) VO_x nanoporous and (b) MnO_x nanofibers. Inset are N_2 adsorption/desorption isotherms of (a) VO_x nanoporous and (b) MnO_x nanofibers.

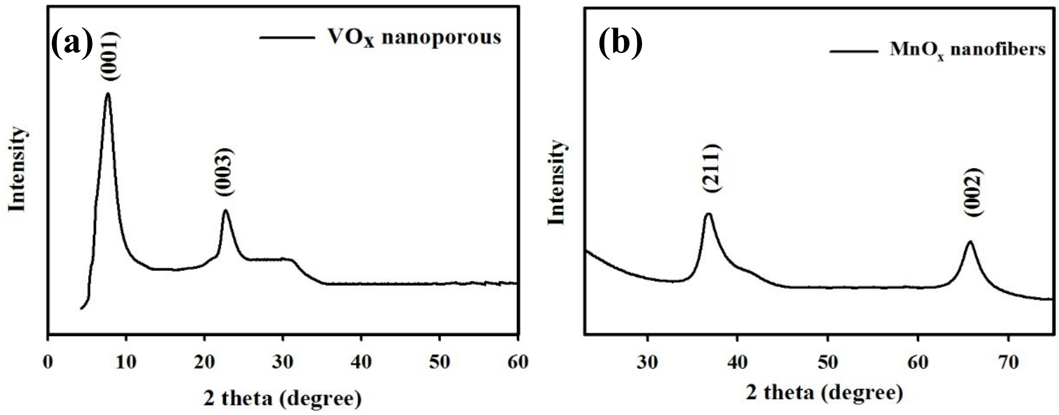

Figure S3. XRD patterns of (a) VO$_x$ nanoporous and (b) MnO$_x$ nanofibers.

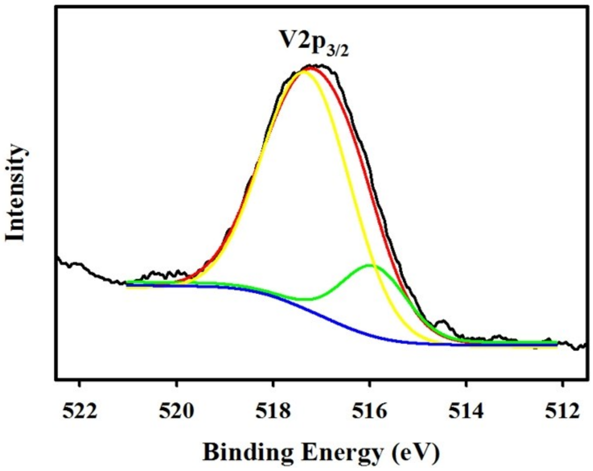

Figure S4. Core-level XPS spectrum of V 2p$_{3/2}$ for a VO$_x$ film.

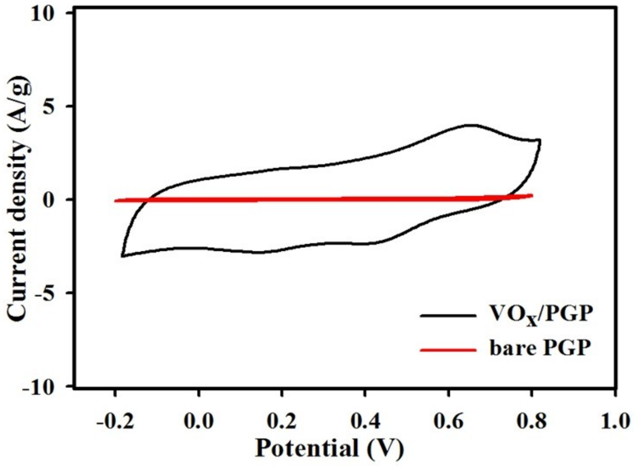

Figure S5. CVs of VO$_x$/PGP and bare PGP electrodes in PLA electrolyte at 5 mV/s.

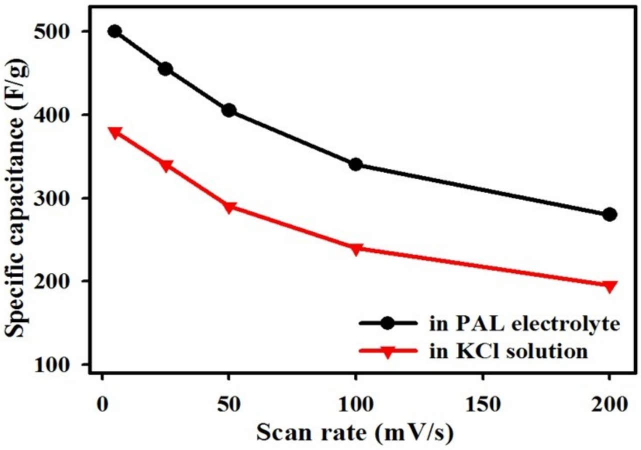

Figure S6. *C_{sp}* retentions of the VO$_x$/PGP electrode in PAL gel electrolyte and in KCl solution as a function of scan rate.

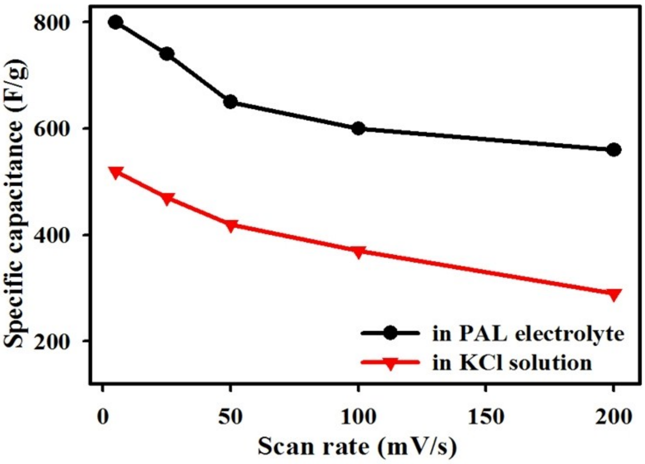

Figure S7. C_{sp} retentions of the MnO$_x$/PGP electrode in PAL gel electrolyte and in KCl solution as a function of scan rate.

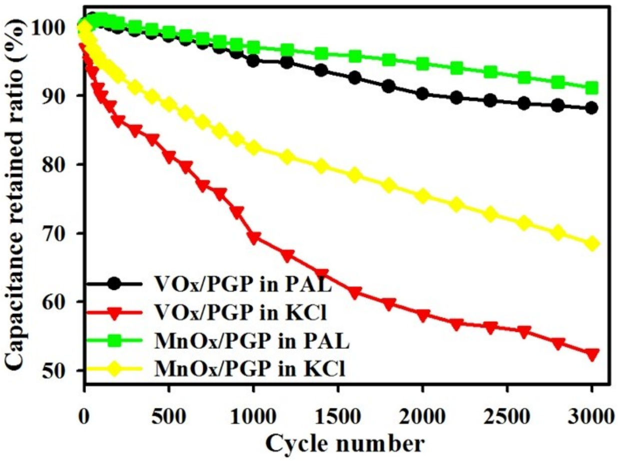

Figure S8. Cycling performance of VO$_x$/PGP and MnO$_x$/PGP electrodes in PAL gel and KCl solution.

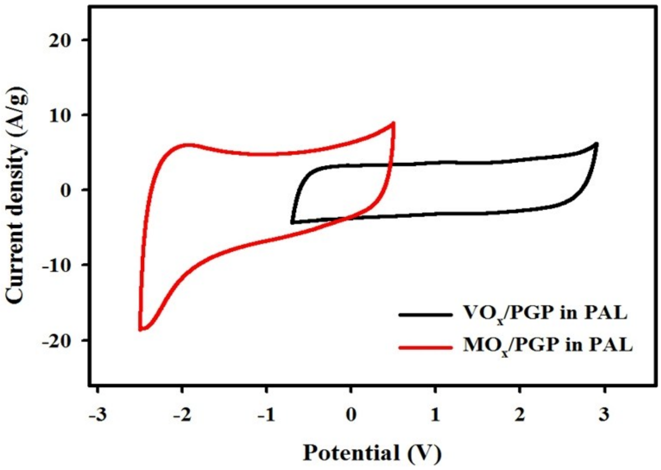

Figure S9. CV curves of the potential limits for VO$_x$/PGP and MnO$_x$/PGP in PAL electrolytes at 5 mV/s.

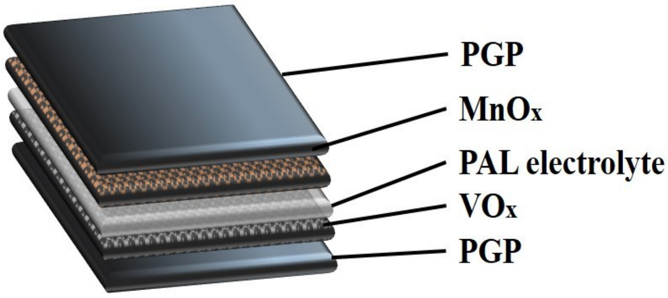

Figure S10. Schematic illustration of the assembled HVWASC devices.

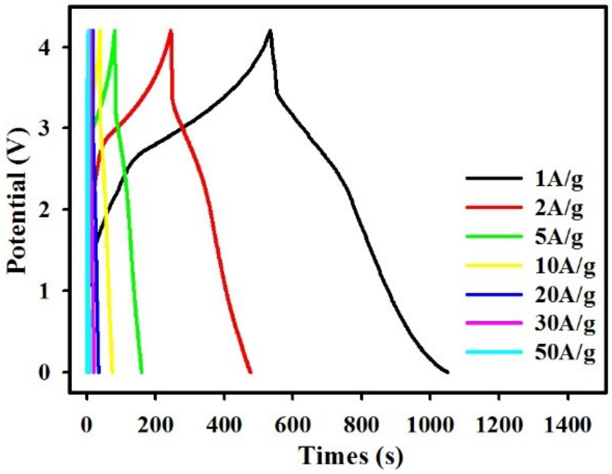

Figure S11. GCD curves of the HVWASC device under various current densities (1−50 A/g)

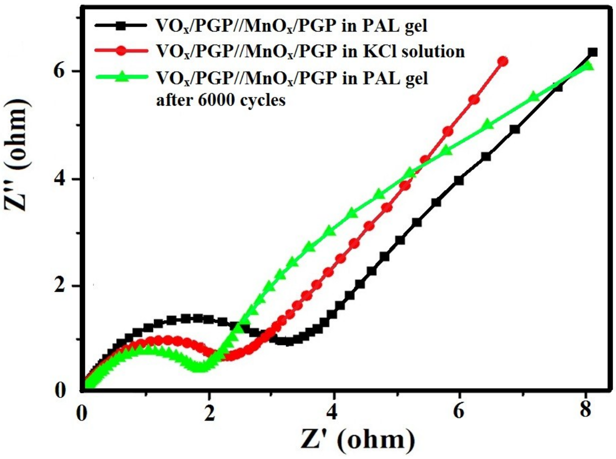

Figure S12. Nyquist plot for HVWASC device using a sinusoidal signal of 5 mV. (Z′ is real impedance. Z″ is imaginary impedance.)

References

1. L. Sun, C. L. Chien and P. C. Searson, *Chem. Mater.,* 2004, **16**, 3125− 3129.
2. Z. Liu, D. Elbert, C.L. Chien and P. C. Searson, *Nano Lett.,* 2008, **8,** 2166–2170.
3. M. J. Deng, C. Z. Song, C. C. Wang, Y. C. Tseng, J. M. Chen and K. T. Lu, *ACS Appl. Mater. Interfaces*, 2015, **7**, 9147−9156.
4. C. Liu, Z. Yu, D. Neff, A. Zhamu and B. Z. Jang, *Nano Lett.,* 2010**, 10**, 4863– 4868.
5. R. B. Rakhi, W. Chen and D. Cha, *Nano Lett.*, 2012, **12**, 2559−2567.